Development of a transfer model for the design and the operation of sodium purification systems for fast breeder reactors

Nayiri Khatcheressian, Latge Christian, Xavier Joulia, Thierry Gilardi, Xuan Mi Meyer

Development of a Transfer Model for the Design and the Operation of Sodium Purification Systems for Fast Breeder Reactors

Nayiri Khatcheressian,[1,2,3]* Christian Latgé,[4] Xavier Joulia,[2,3] Thierry Gilardi[1] and Xuan Meyer[2,3]

1. CEA, DEN, Cadarache DTN/STPA/LIPC, F-13108, Saint-Paul-Lez-Durance, France

2. Université de Toulouse, INPT-ENSIACET, UPS, Laboratoire de Génie Chimique, 4, Allée Emile Monso F-31030, Toulouse, France

3. CNRS, Laboratoire de Génie Chimique, F-31030, Toulouse, France

4. CEA, DEN, Cadarache DTN, F-13108, Saint-Paul-Lez-Durance, France

Operating a Sodium Fast Reactor (SFR) in reliable and safe conditions requires mastering the quality of the sodium fluid coolant, regarding oxygen and hydrogen impurities contents. A cold trap is a purification unit in SFR, designed to maintain oxygen and hydrogen contents within acceptable limits. The purification of these impurities is based on crystallization of sodium hydride on cold walls and sodium oxide or hydride on wire mesh packing. Indeed, as oxygen and hydrogen solubilities are nearly nil at temperatures close to the sodium melting point, i.e., 97.8 °C, on line sodium purification can be performed by cooling down liquid sodium flows and promoting crystallization of sodium oxide and hydride. However, the management of cold trap performances is necessary to prevent from unforeseen maintenance operations, which could induce shut-down of the reactor. It is thus essential to understand how a cold trap fills up with impurities crystallization in order to optimize the design of this system and to overcome any problems during nominal operation. This paper deals with the mathematical modelling of crystallization process in a cold trap and predicts the location and the amount of the impurities deposit, on cold walls for sodium hydride and on wire mesh packing for sodium oxide. A model of the front propagation by "diffuse deposit interface method" was developed and sensitivity to various parameters was evaluated. These results will enable to understand the consequences of the impurities deposited on the hydrodynamics and heat transfer in a cold trap.

Keywords: sodium, Fast Neutron Reactor, cold trap, purification, crystallization

INTRODUCTION

The development of Sodium Fast Reactor (SFR) is possible, thanks to attractive sodium properties. Nevertheless, this coolant needs to be purified because of a potential ingress of impurities mainly oxygen and hydrogen inducing deleterious effects. The main sources of impurities in the secondary sodium loop are due to aqueous corrosion in steam generator inducing hydrogen production and diffusion through tube walls and maintenance operations inducing air and moisture ingress from inert cover gas (argon) and oxygen from structural material. Oxygen ingress induces a limited metal surface corrosion and dissolution of the circuits. In the primary circuit, the radioactive pollution may be caused by corrosion products activated in the core, then carried by the sodium flow and deposited on the internal structures, mainly on cold zones which are consequently contaminated. This implies to decontaminate the structures in order to reduce the dosimetry, when a maintenance operation is decided. It is thus important to keep oxygen content in sodium lower than a concentration around 3 ppm[1] in order to limit corrosion and associated radioactive contamination in the primary circuit. The hydrogen level is required to be less than a concentration of around 0.1 ppm[1] so that a potential sodium water reaction in a steam generator generating hydrogen will be early detected. Higher level would cover small leaks and this might result in propagation into a larger leak and failure of more tubes. Moreover, these pollutants, at very high contents, could also deposit as sodium hydride and oxide on the cold walls of the circuit, which may lead to the plugging of the narrowed sections or the reduction of heat transfer coefficient in heat exchangers. Recently, Kozlov et al.[2] quantified the source of impurities entering the sodium in a fast reactor in all operating regimes of a nuclear plant. Thus, by decreasing oxygen and hydrogen content in sodium coolant, a cold trap appears as a major component in a Sodium Fast Reactor.

On the basis of the works performed by Latgé[3] and related further in this article, it was decided to develop a code aimed to optimize the design and the operation of the sodium purification systems for future SFRs and experimental Na facilities. The model is based on a coupling between hydrodynamics, mass and heat transfer; mass transfer involves nucleation and growth kinetics of crystals. This paper presents an improved mathematical model for the description of the crystallization phenomena of sodium oxide and hydride in the whole volume of the cold trap. As an example, calculation results are given for a simple geometry of cold trap, but the model can be easily adapted to any other cold trap architecture.

A PURIFICATION PROCESS BASED ON CRYSTALLIZATION

The solubilities of oxygen and hydrogen in sodium are very low. They are nearly nil near the sodium melting temperature i.e., 97.8 °C. Noden[4] and Wittingham[5] proposed two correlations to calculate the respective solubilities of oxygen (Equation (1)) and hydrogen (Equation (2)) in sodium as a function of temperature, given in ppm (μg of impurity per g of Sodium).

*Author to whom correspondence may be addressed.
E-mail address: nayirikh@gmail.com

$$\log[O(ppm)] = 6.250 - \frac{2444.5}{\mathrm{T(K)}} \; for\; T(K) = [383; 823] \quad (1)$$

$$log[H(ppm)] = 6.467 - \frac{3023}{T(K)} for T(K) = [383; 673] \quad (2)$$

Thus, crystallization of sodium hydride NaH and sodium oxide Na_2O can occur by decreasing sodium temperature below the saturation temperature. It can be performed in a cold trap in which a heat exchange is carried out. The ingoing liquid metal sodium is cooled down by, for instance, an organic fluid, injected at the bottom of the cooling zone, through an extern shell (Figure 1). Some cold traps can be cooled by other means such as air, Na-K eutectic. To promote heterogeneous crystallization and to trap the sodium oxide and hydride crystals, a support (stainless steel packing) is placed in the cold trap. Purification process by crystallization is achieved by following several steps as shown in Figure 2.

1. The sodium is first cooled down in a heat-exchanger-economizer (at the entrance of cold trap) to a temperature close to the saturation temperature T_{sat} of oxygen and/or hydrogen. C_{in} refers to the inlet impurity concentration.
2. The sodium flows through a cooler where it reaches a crystallization temperature Tc below the saturation temperature of oxygen and/or hydrogen. Crystallization of NaH and Na_2O starts by heterogeneous *nucleation* on surfaces and then progresses by *growth,* as described by Feron, Latgé and Saint-Martin.[6–8]
3. Formed crystals stick to cooled walls (NaH) and/or wire mesh packing (NaH, Na_2O). Thus, oxygen and hydrogen concentrations in the sodium (C) decrease down to a minimum value (C_{out}) at the bottom of the cold trap (Coldest temperature of the Trap: T_{CT}).
4. Finally, the purified sodium (flowing out through the central tube) is heated up through the heat exchanger-economizer.

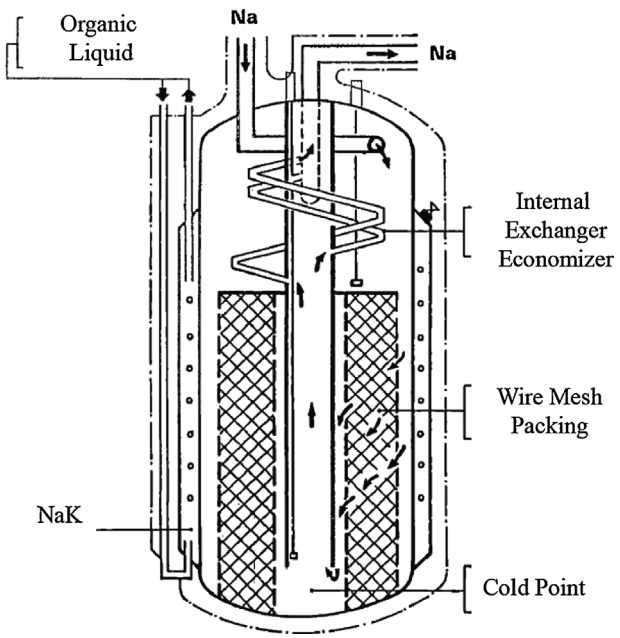

Figure 1. Cold Trap Scheme.

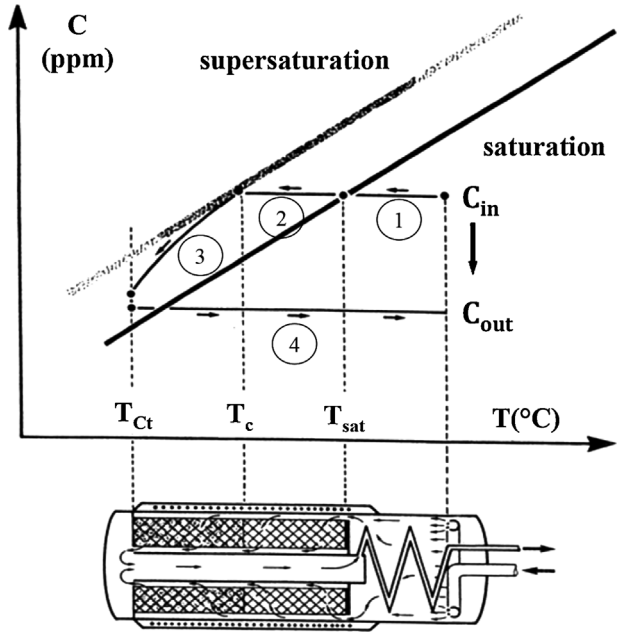

Figure 2. Evolution of impurity concentration C with temperature T.

BACKGROUND OF SODIUM PURIFICATION BY CRYSTALLIZATION ABOUT SODIUM PURIFICATION

Up to now, many cold traps have been designed and operated, and so numerous experimental studies have been carried out. Experimental data are relatively abundant but also diversified depending on the cold trap technology: Fermi cold trap by Yevick[9] and the study of the effectiveness of wire mesh packing, Southwest Experimental Fast Oxide Reactor by Gadeken and Plummer[10] and the evaluation of trapping effectiveness, Prototype Fast Reactor (UK) by Hebditch and Gliddon[11] and the analysis of the deposit on wire mesh, Phenix reactor (France) and the endoscopic examination carried out by Latgé et al.[12] to understand flow reduction, Fast Breeder Test Reactor which allows Rajan[13] to identify some pipe plugging. Experimental data have been reported in detail.[6,14,15] Murase et al.[16] analyze impurities interaction in mesh packing, and Basov et al.[17] investigate the effect of electromagnetic mixing on hydrodynamics and heat transfer among impurities.

Due to the previous operational feedback on cold traps, new concepts have been developed in France. The PSICHOS concept developed for Superphenix reactor is composed of a cooling zone for removal hydride impurities on cold walls and an isothermal packed zone for oxide impurities.[12,18] PIRAMIDE cold trap concept was developed for the European Fast Reactor and different packing sections are disposed as successive trays in order to avoid any mesh plugging.[3]

Meanwhile, computation has also been considered. Goplen et al.[19] simulated dynamical performance of one-dimension cold trap. Dynamical performance of a two-dimension cold trap was simulated by McPheeters and Raue[20] with MASCOT code. A dynamic analysis of sodium purification system to remove sodium hydride impurities was carried out by Kim et al.[21] in Korea. In China, Zhao and Ren[22] developed a theoretical analysis to optimize performances of a sodium cold trap. In Russia, Kumaev et al.[23] developed impurity mass-transfer code. In India, Hemanath et al.[1] used their own code (COCOMO) to understand the effect of various parameters for a PIRAMIDE-PSICHOS mixed

cold trap. Latgé et al.[24] used VISCEN code to predict cold trap behaviour.

In spite of many improvements of cold traps performance achieved from experimental studies or simulation analysis, no-one, except Feron and Latgé,[6,7] distinguished nucleation from growth mechanism in crystallization process. Most research approaches for sodium purification are a mass transfer model, neglecting nucleation and growth mechanisms. Although nucleation mass is definitely insignificant compared to crystals mass, nucleation process keeps a major role on deposits localization, whether it occurs on wire mesh packing or on cold walls, and thus on global efficiency of purification process. Furthermore, couplings physical phenomena and their impacts on thermohydraulics conditions evolution during crystals accumulation are not studied.

However, for cold traps clean of any crystals, growth of the impurities can only occur if nuclei are already formed. Nucleation kinetics fixes ahead the location of future nuclei and thus crystals' one. By modelling the localization of impurities crystals formed inside the cold trap, nucleation kinetics heavily impact its filling, as well as its efficiency. In order to describe a kinetics model as precise as possible, nucleation and growth process should be distinguished.

Experimental studies were carried out in CEA Cadarache, on mock-up[6,8] to understand the basic mechanisms of crystallization of sodium oxide and sodium hydride and to establish their respective nucleation and growth kinetics as described by Latgé.[3] These equations have been established for crystallization on wire mesh packing. The general form of crystallization kinetics $\dot{m}_V$, given for one impurity O or H, in $[kg_{Na2O}/(s.m^3)]$ or $[kg_{NaH}/(s.m^3)]$, are

$$\dot{m}_{V,i}^{X} = a_i^X \exp\left(-\frac{E_i^X}{RT}\right) Sv_i^X(t) \left[\frac{C_i(T) - C_{sat,i}(T)}{10^{-6}\rho_{Na}}\right]^{n_i^X}. \quad (3)$$

In this equation, index X refers to Nucleation (N) or growth (G) and index i refers to the impurity (NaH or Na_2O). a is the rate constant (kg/ (s.ppm n^x.m^2)), E is the activation energy (J/mol), R is the perfect gas constant (J/(mol.K)), Sv is the crystallization volumic surface of reference (m^2/m^3) (wire or walls for nucleation, nuclei and crystals for growth), n_X is the order of the crystallization process, C*(kg/m^3) is the saturation concentration for a given temperature calculated by the solubility law, ρ_{Na} is the sodium density in (kg/m^3) and (C-C*) is the supersaturation at temperature T(K). Values of activation energies and kinetics orders are given Table 1.[1]

CRYSTALLIZATION ON WALLS AND ON WIRE MESH PACKING MODELLING

The experimental sodium loop ECRIN includes two parallel test sections, each containing a simple, easily removable experimental cold trap. Impurities are introduced by dissolving the deposits contained in an auxiliary cold trap. The oxygen/hydrogen contents at the inlet of the two test sections are determined by the cold point temperature in the auxiliary trap. Then the oxygen/hydrogen contents in the sodium are measured by a plugging meter (and for some tests by oxygen-meter and hydrogen-meter). Sodium oxide/hydride crystallization is induced in a narrow flow section by cooling the sodium at a linear rate, this reducing the flow rate. Then, in successive temperature steps, the saturation temperature is determined for which no mass transfer occurs between the solid and dissolved phases. The two experimental cold traps are drained, and then examined in a glove box under argon atmosphere, to observe the distribution and appearance of the deposits. Samples are taken, part for scanning electron microsopy, part for quantitative chemical analysis of the compounds.

Experiments carried out in facility EPINAR have unexpectedly revealed that for a cold trap designed with an upper unpacked cooled zone, sodium hydride crystallization occurs preferentially on cold walls of the system (Figures 3 and 5) whereas sodium oxide crystallization occurs only on wire mesh packing (Figures 4 and 6) as explained by Latgé et al.[3,12,24] This has been partly explained by the fact that growth rate of Na_2O is limited by the diffusion of O^{2-} in the boundary layer whereas the growth rate of NaH is limited by the integration step of the H^- ion in the crystal lattice. However, in the case of a non-optimized unpacked cooled zone, hydride might crystallize on wire mesh packing located down-stream as well. Thus, co-crystallization might occur between sodium hydride and sodium oxide. Sodium hydride and sodium oxide can be distinguished by chemical analysis and sometimes by their colour.

Whether it deals with crystallization on wire mesh or crystallization on cold walls, crystallization developed models tackle with porous medium problematic. Indeed, if it sounds trivial that wire mesh packing filling with impurities can be

Table 1. Activation energies and process orders of sodium oxide and sodium hydride

Process	Nucleation (N)		Growth (G)	
Impurity	Na_2O	NaH	Na_2O	NaH
E (kJ/mol)	−60	−450	−45	−43.6
n	5	10	1	2

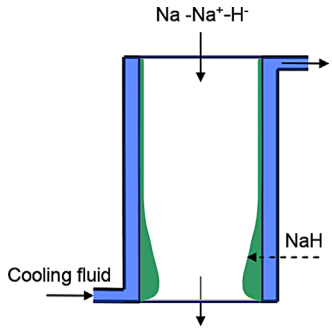

Figure 3. Trapping schemeof NaH on cold walls.

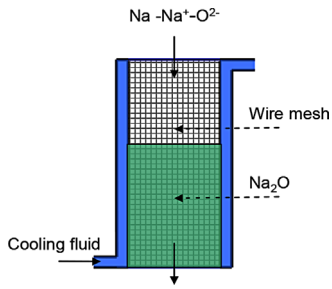

Figure 4. Trapping scheme of Na_2O on wire mesh.

Figure 5. Trapping experimental results of NaH on cold walls.

Figure 6. Trapping experimental results of Na_2O on wire mesh.

considered as a porous medium (Figure 6), experimental analysis revealed that crystals formed on cold walls consisted of static sodium–hydride crystals mixture with a certain void fraction (Figure 5). Experimental images have been taken thanks to endoscopic examination of the trap.

The proper porosity of the system is initially equal to one (liquid sodium porosity) if the deposit only occurs on walls (NaH) and equal to the void fraction of the mesh packing if the deposit occurs on wire mesh (Na_2O/NaH).

However, besides porous medium problematic, crystallization model on cold walls is dealing with another problematic: the interface tracking. The interface progression depends on impurities accumulation on walls and its localization comes as a key parameter of the model. On one hand, deposit tracking enables to establish where nucleation and then growth of the impurities can occur. On another hand, it enables to apprehend the evolution of the internal trap's geometry which corresponds to the free path of sodium flow within the upper plenum of the cold trap.

As a results, crystallization models which have to be developed to apprehend sodium oxide and sodium hydride deposits on cold traps refer to different behaviours regarding their corresponding location (Table 2).

Table 2. Implemented models in crystallization processes

Crystallization	Wire mesh packing	Cold walls (packless zone)
Impurities	–Na_2O -NaH	– NaH
Models	–Porous medium densification	– Porous medium densification - Interface tracking
Surface to crystallize	–Wire mesh -Oxide and/or hydride crystals	– Hydride crystals

Porous Medium Densification Model

Porosity ϕ evolution highlights the filling of cold traps with impurities and impacts inevitably physical phenomena transfer. The system composed of metal liquid sodium, oxide and/or hydride crystals and wire mesh, in case of packing zone, is considered as an isolated mixture whose physical properties are mathematical consequences of the compounds properties.

To describe the intern evolution of the cold trap, mass conservation equation is coupled with the transfer equations for each phase (sodium liquid phase/solid mesh-crystals phase). Assumptions have to be considered to establish the system of conservation equations:

- Stream flow and heat transfer are axisymmetric and bidimensionnal (no azimuthal variation).
- Thermohydraulic fluid behaviour is assumed to be ideal and its properties are evaluated at the cell temperature. However, fluid density is linearly dependent on gravitation force term in the Navier–Stokes equation (Boussinesq approximation).
- Heat radiation can be neglected (sodium emissivity of 0.05).
- Viscous dissipation and work of pressure stress can be neglected in Energy equation.
- Liquid/Solid local thermal equilibrium is assumed.
- Sodium fluid is entering the trap section at a one temperature.
- Crystal phase is assumed to be hooked up to the mesh, solid phase velocity is null.

Mass conservation law

Be n_{imp} the number of impurities introduced in the system. The porosity ϕ is defined as the void fraction occupied by the liquid phase, supposed as incompressible (sodium liquid metal) through the porous medium. Mass conservation on liquid phase on an infinitesimal volume imposes

$$\frac{\partial \phi}{\partial t} + div(\phi \vec{v}) = -\frac{1}{\rho_{Na}} \sum_{i=1}^{n_{imp}} \left(\bar{m}^{N}_{V,i} + \bar{m}^{G}_{V,i} \right). \quad (4)$$

Mass conservation on solid phase (mesh and crystals) directly determines the porosity of the system with

$$\frac{\partial \phi}{\partial t} = -\sum_{i=1}^{n_{imp}} \left(\frac{\bar{m}^{N}_{V,i} + \bar{m}^{G}_{V,i}}{\rho_i} \right). \quad (5)$$

Momentum conservation law

Continuum equation governing the conservation of momentum in binary phase change cold trap system is assumed only on the

sodium liquid phase. It involves volume forces $\vec{q_V}$ [kg/(m^2.s^2)] and surface forces $\overline{\overline{\Im}}$ [kg/(m.s^2)] such as pressure and viscous stresses. It is expressed as

$$\phi\rho_{Na}\frac{\partial\vec{v}}{\partial t}+(\phi\rho_{Na}\vec{v}).\overline{\overline{grad}}\,\vec{v}=\vec{q_V}+div(\phi\overline{\overline{\Im}})+\left[\sum_{i=1}^{n_{sel}}(\bar{m}_{V,i}^{N}+\bar{m}_{V,i}^{G})\right]\vec{v}. \tag{6}$$

Volume forces $\vec{q_V}$ implies gravitational and drag porous medium forces. It comes

$$\vec{q_V}=\phi\rho_{Na}(T)\vec{g}\,[1-\beta_{Na}(T-T_{CT})]-\left[\phi\frac{\mu_{Na}(T)}{k_{mesh}(\phi)}\vec{v}\right]. \tag{7}$$

In Equation (6), v refers to the liquid velocity (m/s). In Equation (7), g [m/s^2] refers the gravity acceleration, β_{Na} [1/K] is the sodium thermal dilatation, μ_{Na} [kg/(m.s)] is the sodium viscosity and k_{mesh} [m^2] corresponds to the mesh permeability.

Energy conservation law

Continuum equation governing the conservation of energy in binary phase change cold trap system is expressed at one local temperature T assuming a local thermal equilibrium between liquid and solid phases:

$$T=T_{(S)}=T_{(L)}. \tag{8}$$

It comes

$$\begin{aligned}(\rho c_p)_{eff}\frac{\partial T}{\partial t}+(\rho_{Na}c_{pNa})\vec{v}.\overline{grad}(T)\\ =div(\lambda_{eff}\overline{grad}T)-\sum_{i=1}^{n_{sel}}\left(\bar{m}_{V,i}^{N}+\frac{\bar{m}_{V,i}^{G}}{M_i}\right)\Delta h_{fu,i}^{o}(T).\end{aligned} \tag{9}$$

In this equation, the index "eff" refers to the liquid/solid pro rata regarding the porous medium, c_p[J/(kg.K)] is the heat capacity, λ [W/(m·K)] is the thermal conductivity, M [kg/mol] corresponds to the molar mass and Δh_{fu}^{o} [J/mol] is the latent heat of fusion.

Impurities conservation law

Continuum equation governing the conservation of species in binary phase change cold trap system is expressed on dissolved impurities as

$$\frac{\partial(\phi C_i)}{\partial t}+\vec{v}.\overline{grad}(C_i)=div(D_{i,eff}\overline{grad}C_i)-\sigma_{M,i}\left(\bar{m}_{V,i}^{N}+\bar{m}_{V,i}^{G}\right). \tag{10}$$

This system of [4 + n_{imp}] conservation Equations (4)–(6), (9), and (10) describes the model (Khatcheressian)[25] of porous media densification, result of deposits accumulation.

INTERFACE TRACKING MODEL

Sodium hydride crystallization on cold walls, as well as crystallization on packing, is dealing with porous media issues. Former equations remain thus the same. Fundamental difference between these two models is on the management of the localization of impurities crystallization. For a wire mesh packing system, nucleation and growth occur through the entire described volume, as soon as supersaturation has been reached (Figure 2). But because of the heterogeneous nucleation characteristic, impurities crystallization in a packless cooling zone can only occur on walls or crystals deposit already formed (Figure 3). Thus tracking the interface is essential: it describes evolution over time and through space, in order to assign where nucleation occurs.

Localization of the interface deposit. Over the past fifteen years, a class of numerical techniques known as level set[26–29] or phase-field[30–32] methods has been built to tackle some of the most complex problems in fluid interface motion. Whether it is from a mathematical point of view or physical ones, these models introduce a diffuse interface model. Diffuse interface models assume that the interface between the phases is not a sharp boundary, but has a finite width and is characterized by rapid but smooth transitions. This model enables to avoid convergence problems linked to interface discontinuities.

A variable Ψ is introduced to describe the occurrence rate of the crystallization. It has a constant value in the bulk phase to locate them over the domain. Indeed, $\Psi=0$ corresponds to the liquid sodium phase whereas $\Psi=1$ corresponds to the deposit phase (Figure 7). Then Ψ varies smoothly across the interface region in a hyperbolic tangent (Figure 8). The tracking of the surface $\Psi=0.5$ apprehends the propagation of the interface, resulting of the crystals accumulation.

If the volumic surface (Equation (3)) offered to crystals growth Sv^G are nuclei and former crystals, the volumic surface offered to nucleation Sv^N is function of variable Ψ. Nucleation process only occurs for $\Psi>0$.

A diffuse interface as the nucleation zone. In the model of crystallization on wire mesh packing, heterogeneous nucleation is assumed to occur on the stainless steel wire mesh. It is a primary nucleation whom initial volumic surface remains the packing density. In this model, secondary nucleation on crystals formed is not considered. Indeed, nucleation process keeps its major role in localizing the impurities deposit. Any mass created by a secondary nucleation can be neglected regarding the mass created by growth.

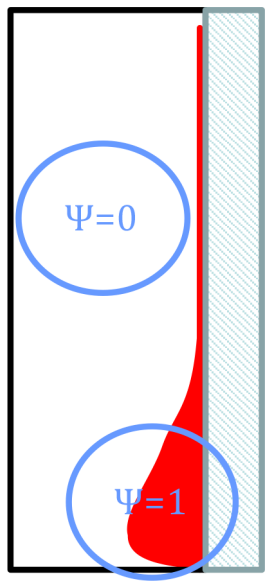

Figure 7. Phases localization with occurring rate variable Ψ.

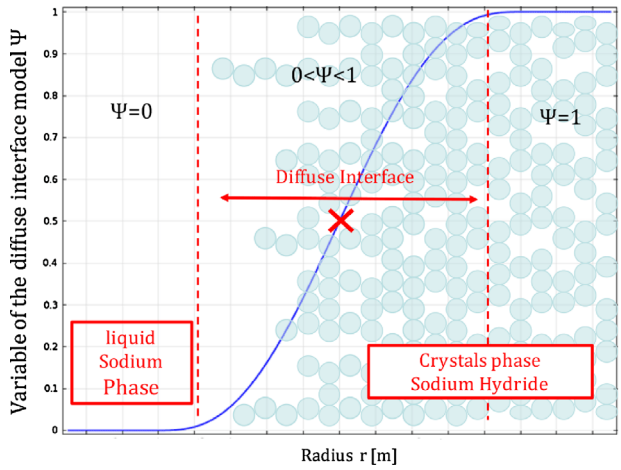

Figure 8. Occurring rate Ψ through diffuse interface.

If nucleation enables to localize crystals deposition, these models assume that the densification of the volume comes from the crystal growth.

Thus, on the model of crystallization on packless cooling zone, if primary nucleation occurs on cold walls, secondary nucleation keeps a sense since the deposit is constantly moving, regardless supersaturation conditions. Initiating growth impurities crystallization, nucleation process occurs on the top surface of the deposit and keeps a Gaussian profile as shown in Figure 9. Indeed, upfront deposit, nucleation kinetic is null because of the lack of crystal support to initiate crystallization. For a given thickness of deposit reached nucleation kinetic stops because of an insufficient supersaturation. A compromise exists between crystals surface and supersaturation for which nucleation kinetics is the highest.

The volumic surface offered for nucleation of the impurities, on the model of crystallization on packless cooling zone, is a function of the density of crystals over the region it occurs.

Since without any nuclei supply, deposit stops progressing but only gets denser thanks to crystal growth, secondary nucleation can be viewed as the driving force. Nucleation is thus responsible for the diffuse interface motion. As a result, the thickness where nucleation occurs is assimilated to the diffuse interface length e_Γ. This assumption enables to directly establish the volumic surface for nucleation on this model with

$$Sv^N = \frac{\psi}{e_\Gamma}. \tag{11}$$

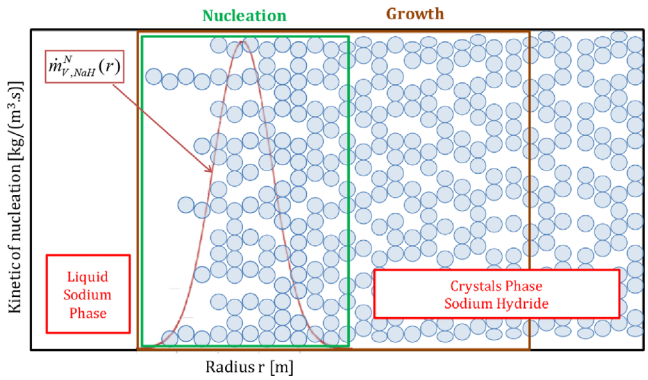

Figure 9. Location of the nucleation process.

Velocity front propagation. Before any start of deposit progress, the first crystals layers formed on cold walls must get denser. It is assumed that it corresponds to the diffuse interface length since nucleation is initiating the motion of the interface. Thus, hydride deposit will not progress until a first critical porosity profile $(\partial\phi/\partial r)_{crit}$ has not been reached. The front velocity is then defined such that porosity profile over the diffuse interface remains the same. It comes

$$\forall(r,z)/0 < \psi(r,z) < 1 : \frac{D\phi}{Dt} = \frac{\partial\phi}{\partial t} + \vec{v}_{FS}\left(\frac{\partial\phi}{\partial r}\right)_{crit} = 0. \tag{12}$$

For a given z position in cold trap, radial growth crystallization is assumed. Front velocity field is thus expressed as

$$v_{FS}(r) = \frac{\partial\Phi(r)}{\partial t} \Big/ \left(\frac{\partial\phi}{\partial r}\right)_{crit}. \tag{13}$$

Equation (13) can be simplified with the approximation of a linear porosity profile over the diffuse interface. $(\partial\Phi/\partial r)_{crit}$ is then assigned as a constant.

Surface quantity conservation. As soon as crystallization occurs, the thickness of the deposit rises and the porosity field of the system "packless cooling zone" changes. Deposit interface progresses at the crystallization front velocity. Its spatiotemporal evolution is mathematically expressed as a convection equation which conveys the surface quantity conservation:[28,29,33]

$$\frac{\partial\psi}{\partial t} + \overrightarrow{v_{FS}} \cdot \nabla\psi = \eta\nabla \cdot (e_\Gamma \nabla\psi) - \eta\nabla \cdot \left[\psi(1-\psi)\left(\frac{\nabla\psi}{|\nabla\psi|}\right)\right]. \tag{14}$$

Left-side terms apprehend the convection equation from which the variable Ψ is transporting at the front velocity v_{FS}. Right-side members are numerically introduced in order to conserve the occurrence rate. The first right member corresponds to a numerical diffusion term in order to keep the length of the diffuse interface constant and equal to its initial value. The second term corresponds to a numerical flux, introduced to maintain the interval bounds strictly between 0 and 1. On this equation, the parameter η(m/s) represents a readjustment velocity, assigned as the average front velocity.

This equation of surface quantity conservation is added to the system of equations in porous medium. This system of $[5 + n_{imp}]$ conservation Equations (4)–(6), (9), (10), and (14) describes the model of crystallization on packless cooling zone.

SIMULATION AND RESULTS

The mathematical models previously described are discretized and then solved by finite element method in Comsol Multiphysics® software and compared to experimental runs previously performed in CEA Cadarache, France.

Crystallization Conditions on Mockup EPINAR

Experimental studies on wire mesh packing crystallization and cold walls, in CEA Cadarache, have been performed on EPINAR mock-up (Figure 10) by Saint-Martin and Latgé.[6,12,24] EPINAR is a two meters length cold trap. The upper part of one meter length, is designed as a cooling zone in which the inlet sodium (T_e) is

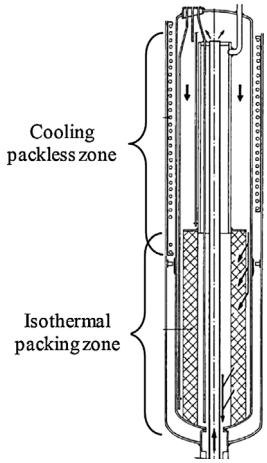

Figure 10. EPINAR mock-up scheme.

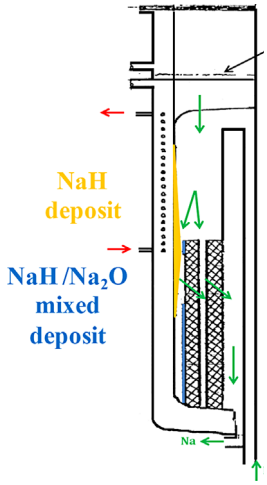

Figure 12. Localization of the impurities on EPINAR experimental test.

cooled down to its coldest temperature T_{CT}. The lower part is designed as an isothermal wire mesh packing zone in order to get a residence time bigger over the coldest zone (at T_{CT}) and then increase the purification efficiency, more particularly for sodium oxide trapping. Figure 11 presents the temperature profile over the mock-up trap.

During one month (673 h) of experiment, a concentration of oxygen corresponding to a temperature of saturation equal to 142 °C (2.75 ppm) and a concentration of hydrogen corresponding to a temperature of saturation equal to 140.5 °C (0.16 ppm) are introduced. Injections of hydrogen and oxygen have been conducted at the same time.

The mock-up trap that served for this experiment is slightly different from the one presented in Figure 10 since the packed zone is filled up with two concentric paralleled wire mesh samples (Figure 12).

After performing an endoscopy, it appeared that sodium hydride preferentially crystallizes on cold walls, in the upper part of the trap as shown on (Figure 12). However, if the efficiency of the sodium hydride crystallization is not at its maximum (=1) on the upper part, some can still crystallizes on the top part of the wire mesh packing. The wire mesh packing zone is mainly devoted to sodium oxide crystallization. Co-crystallization between the two impurities may occur.

Purification analyses of EPINAR test are resumed on Table 3.

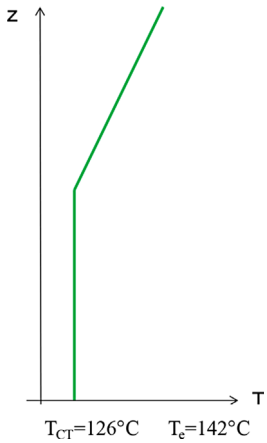

Figure 11. Temperature profile along EPINAR test.

Assumptions and Validation of Crystallization Models

Before any simulation run, the model of crystallization developed on the packless cooling zone required some assumptions. The conservation of the occurrence rate (Equation (14)) required precisely

- The critical porosity profile $(\partial\Phi/\partial r)_{crit}$;
  Until this porosity profile as not been reached, deposit on walls is not progressing. The velocity of the front is then defined such that the diffuse interface keeps its density constant. The profile is set as a constant value that impacts the final value of the thickness, (denominator of the front velocity). In order not to exceed 3 cm after 673 h of test, simulations runs fixed its value to 0.01 m^{-1};
- The thickness of the diffuse interface e_Γ;
  The diffuse interface represents the surfacing of the deposit, and the way it fills with impurities determines the front progressing. The thickness of the diffuse interface is assigned as the thickness in which the impurities nucleate. Simulations runs enabled to visualize a thickness of 5 mm (Khatcheressian);[25]
- The readjustment velocity η;
  The readjustment velocity is such that it keeps constant the thickness of the diffuse interface, as well as the bounds of the variable Ψ strictly between [0,1]. It is assigned as the average velocity of the front:

$$\eta = \frac{1}{2}\left(\frac{1,5cm}{673h}\right) = 3.10^{-9} m/s.$$

In case of co-crystallization of the impurities, it is assumed that one species can nucleate on any surface that which does not belong to its own species. This assumption is expressed through the volumic surface of the specie 'i' as a function which depends not only from the wire mesh but from the crystals growth specific surface of the specie 'j':

$$Sv_i^N(t) = f[Sv_{j\neq i}^G(t)]. \quad (15)$$

Table 3. EPINAR test results

Impurity	NaH	Na_2O
Cumulated Mass	2.05 kg	3.57 kg
Maximal hydride wall deposit thickness	3 cm	/
Average hydride wall deposit thickness	1.5 cm	/
Height of hydride wall deposit	1.5 m	/

Table 4. EPINAR simulation results

Test	Experimental	Simulation
NaH Mass on cold walls	/	1.02 kg
NaH Mass on wire mesh packing	/	1.06 kg
cumulated mass of NaH	2.05 kg	2.08 kg (+1.4 %)
cumulated mass of Na_2O	3.5 kg	3.44 kg (−1.7 %)

Purification analyses of simulation run are compared with experimental ones on Table 4. The models of crystallization give a really good approximation of the expected mass with less that 1.7 % error.

Beside the fact that these models faithfully evaluate the crystallized mass of sodium oxide and sodium hydride, they enable to trace the location of the deposits through their porosity or mass profiles. On the packed zone, the model of $[4 + n_{imp}]$ conservation equations is assumed whereas on the bulk zone, it is the model with $[5 + n_{imp}]$ conservation equations which involves the front motion equation. Thus, the variable Ψ does not exist on the packed zone. The porosity of the trap is so defined:

- On the packed zone, by the mass conservation equation from the $[4 + n_{imp}]$ system equations
- On the bulk zone, by the mass conservation equation from the $[5 + n_{imp}]$ system equations

Figure 13 traces NaH deposit only over the bulk zone, through the porosity profile resulting from the $[5 + n_{imp}]$ system equations. NaH and Na_2O impurities deposits occur as well over the packed zone, as shown in Figures 14 and 15, through their respective mass resulting from the $[5 + n_{imp}]$ system equations.

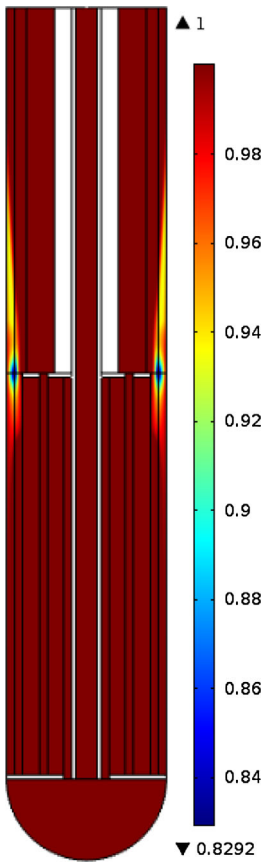

Figure 13. Porosity profile of the cooling packless zone.

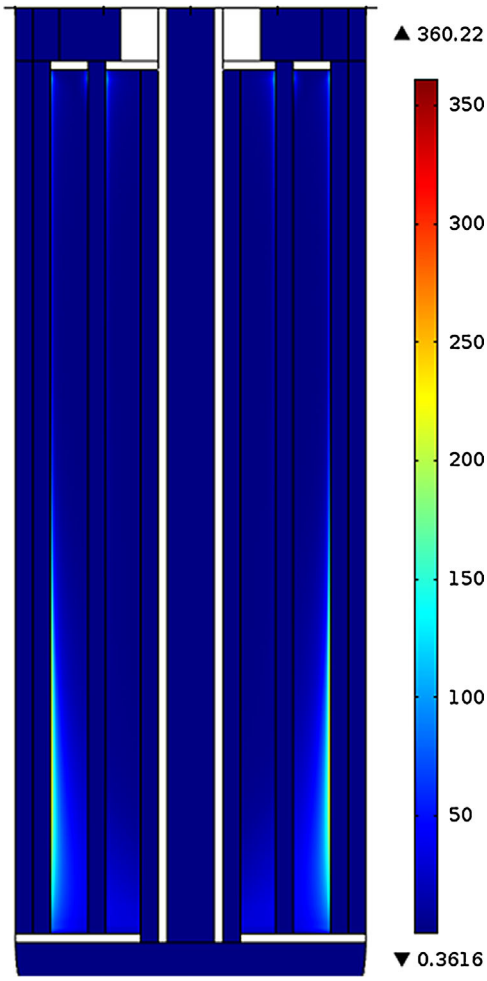

Figure 14. NaH mass (kg/m^3) on wire mesh packing zone.

Simulation enables to distinguish each impurity from another (Figures 14 and 15). Both oxide and hydride deposits on the extreme top part of the wire mesh assured co-crystallization occurred, even if sodium hydride kinetics is much faster than sodium oxide kinetics.

In Figure 13, the porosity field of the packless cooling zone is presented. For $\Phi < 1$, it corresponds to the hydride deposit crystallized on the cold walls. Figures 14 and 15 focus on the wire mesh packing zone and present respectively sodium hydride and sodium oxide crystals density. This simulation gives good results according to what was expected in Figure 12. This point is one of the major advantages of this simulation tool since users can figure out if the trap is plugged or not.

OPTIMIZATION APPROACH FOR HYDRIDE CRYSTALLIZATION ON COLD WALLS

An electromagnetic pump is forcing the sodium fluid, which has been deviated from its main loop, to pass through the cold trap. Through the purification loop, for industrial designs, the fluid can get a maximum flowrate of 30 m^3/h whereas it is circulating at 400 m^3/h over the main loop. For a 1 m diameter trap design, the fluid velocity is rather low, with only 0.2 cm/s. Because of the temperature gradient, the fluid can thus, be subjected to a natural circulation. A natural circulation enables fluid recirculations into the trap and in a certain extend a better purification according to

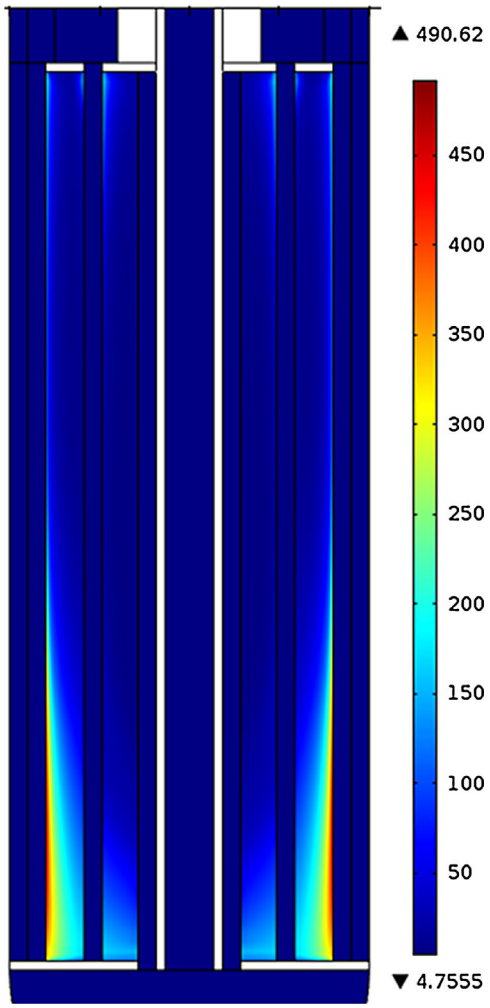

Figure 15. Na_2O mass (kg/m^3) on wire mesh packing zone.

the purification efficiency defined as

$$\varepsilon = \left[\frac{C_{in} - C_{out}}{C_{in} - C_{sat}(T_{CT})}\right] \leq 1. \quad (16)$$

If natural circulation is then required in purification process, the forced circulation is as well important. Indeed, a too low inlet flowrate would not supply a sufficient amount of impurities into the trap to get the proper purification velocity which is industrially specified. Since these two phenomena are on opposition, it exists an optimum of purification to reach, depending on design and operating conditions that is defined from natural and forced circulations.

A Purification Controlled by Flow Circulations

The purification models by crystallization imply a strong interaction between physical phenomena. Indeed, if thermo hydraulic conditions influence impurities crystallization, crystals deposits determine streamline and heat flux distribution. However, these phenomena are controlled by the purification operating parameters on one part and on another part, the cold trap design itself. A non optimized conception could detract a proper management of the trap (purification rate and loading rate). To optimize purification process, the relation between operating and conception parameters on purification criterion

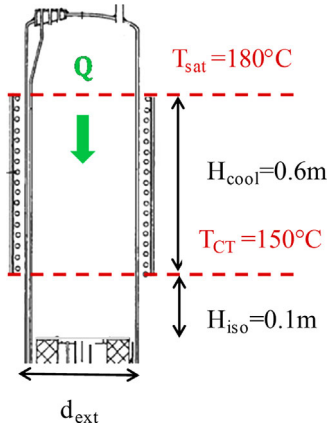

Figure 16. Packless cooling trap concept.

must be analyzed. Since, hydrogen remains the main impurity in the secondary loop during normal operation, purification optimization is investigated for a simple packless cooling trap concept (Figure 16). Sodium cooling is imposed linear from the temperature of saturation down to the temperature of the coldest point. H_{cool} corresponds to the cooling height whereas H_{iso} corresponds to the isothermal height.

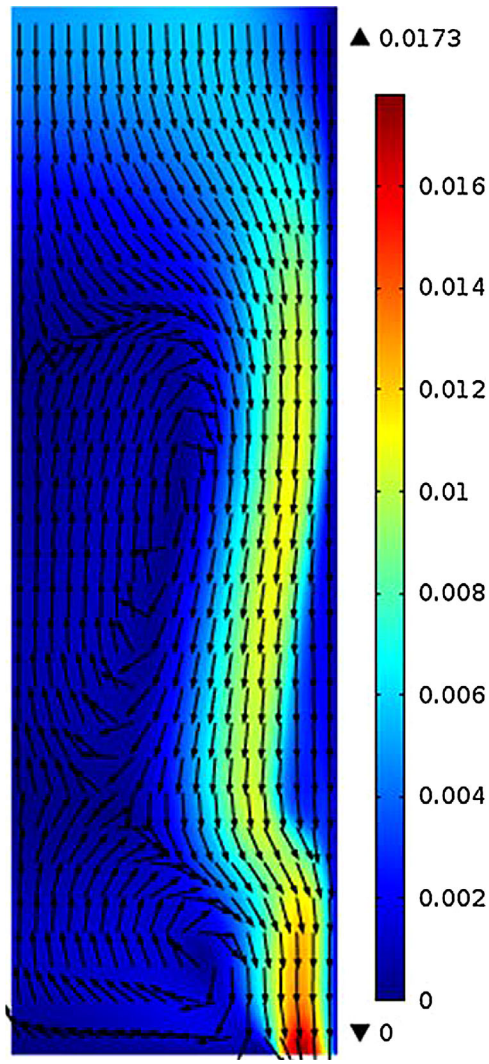

Figure 17. Velocity field WITH Buoyancy force.

Thermohydraulic coupling conditions are principally expressed from Navier–Stokes Equation (6) by the buoyancy volume force $\beta\rho g(T - T_{CT})$. In order to understand the impact of thermal and hydraulic physical phenomena coupling, simulation runs are performed with (Figures 17 and 18) and without (Figures 19 and 20) buoyancy force. For this latter, the force is deliberately disabled. Simulation results are given from a 2D axisymmetric cut.

Hydrogen content (0.62 ppm–Tsat = 180 °C) is introduced during two months of test, with a sodium flow rate of 3 m^3/h. The coldest point is set to 150 °C (0.224 ppm). Cooling profile is linear on 60 cm height. It turned out that a sodium recirculation (Figure 17) pushed the fluid to mainly flow by cold walls, which heavily improves hydride crystallization (Figure 18). When the fluid is only subject to a forced convection (Figure 19), crystallization on walls barely occurs (Figure 20).

These simulation results highlight that purification optimization can be approached for a precise mixed convection which corresponds to a specific management and trap design relation. Without considering crystallization terms, adimensional Navier-Stokes formulation gives

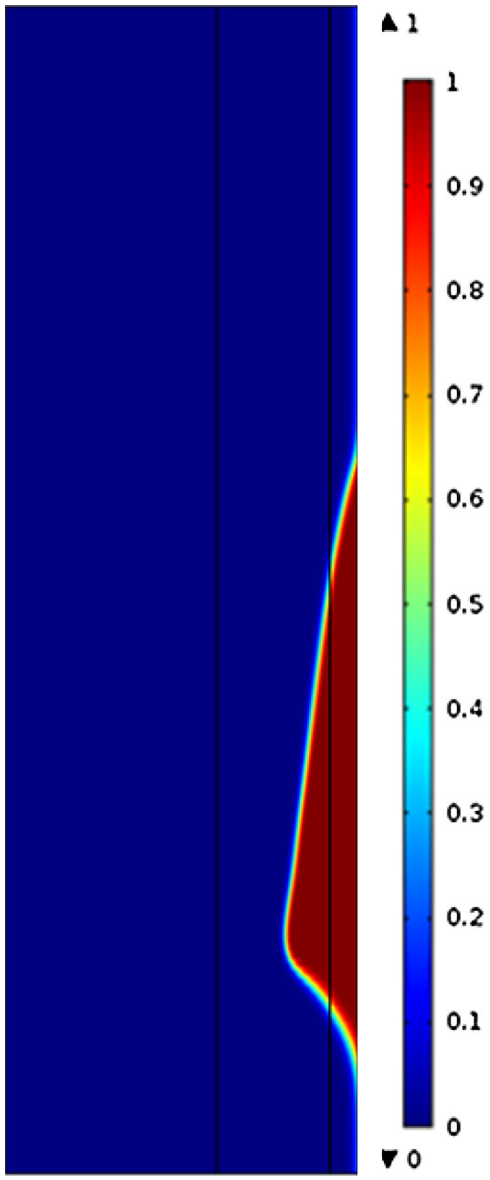

Figure 18. Occurrence rate field WITH Buoyancy force.

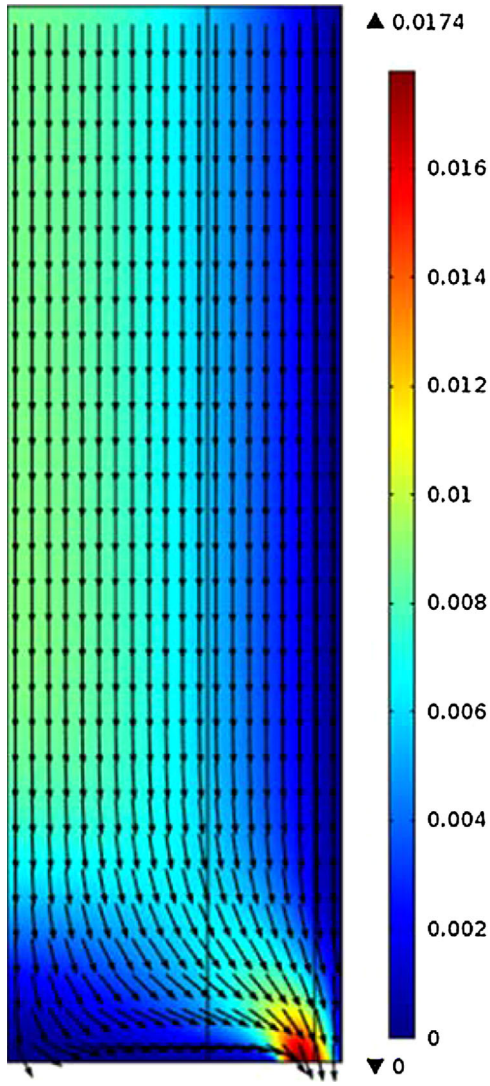

Figure 19. Velocity field WITHOUT Buoyancy force.

$$\frac{\partial v_z*}{\partial t^*} + v_r * \frac{\partial v_z*}{\partial r^*} + v_z * \frac{\partial v_z*}{\partial z^*} = -\frac{\partial p^*}{\partial z^*} + Ri.T^* + \frac{1}{Re}\left[\frac{1}{r^*}\frac{\partial}{\partial r^*}\left(r^*\frac{\partial v_z*}{\partial r^*}\right) + \frac{\partial^2 v_z*}{\partial^2 z^*}\right]. \quad (17)$$

The adimensional buoyancy force highlights the Richardson criterion, function of geometry and operating parameters with

$$Ri = \frac{g\beta(T_{sat} - T_{CT})H_{cool}}{\left(\frac{4Q}{\pi d_{ext^2}}\right)^2} = \frac{\pi^2 g\beta(T_{sat} - T_{CT})H_{cool}{d_{ext}}^4}{16Q^2}. \quad (18)$$

Richardson number characterizes the ratio of natural convection over forced convection. Its study should enable to adapt operating and design conditions in order to optimize purification requirements.

Purification Optimization for a Simplified Case

Purification optimization in industry depends on requirements. However, for this study, purification process will require to maximize two criteria: efficiency ε and deposit mass m_{NaH}. Indeed,

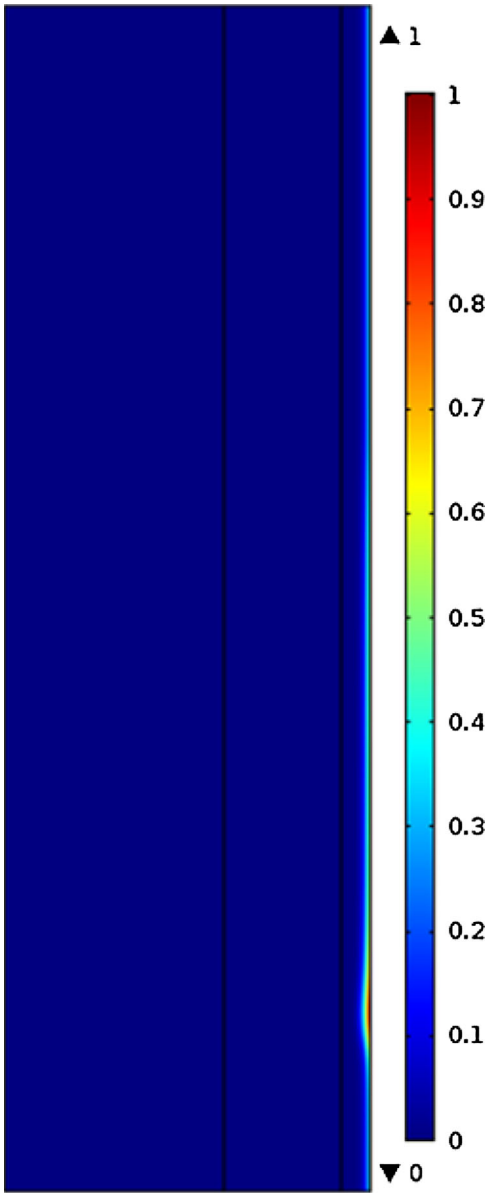

Figure 20. Occurrence rate field WITHOUT Buoyancy force.

if most of hydrogen crystallizes on walls, the purification is efficient. It thus enables to keep free the wire mesh packing for oxygen trapping. Furthermore, the most important is the hydrogen deposit mass on walls and the shortest is the purification campaign. These two aspects lead to define a global criterion with the relation ξ_p:

$$\xi_p = \varepsilon \frac{m_{NaH}}{m_{\max,NaH}} = \left[\frac{C_{in} - C_{out}}{C_{in} - C_{sat}(T_{CT})}\right]\left[\frac{m_{NaH}}{m_{\max,NaH}}\right] \leq 1. \qquad (19)$$

In this relation $m_{\max,NaH}$ corresponds to the maximum mass that is obtained over the different simulation runs. The present study proposes an optimization approach by tackling on the specific parameters couple defined by Richardson number. Optimizing purification process can be obtained while maximizing the purification criterion ξ_p, with, for instance, the parameters couple (d-Q) defined by the relation d_{ext}^4/Q^2 (Equation (18)). In this study, the flow rate Q varies from 1 m^3/h to 5 m^3/h whereas the diameter

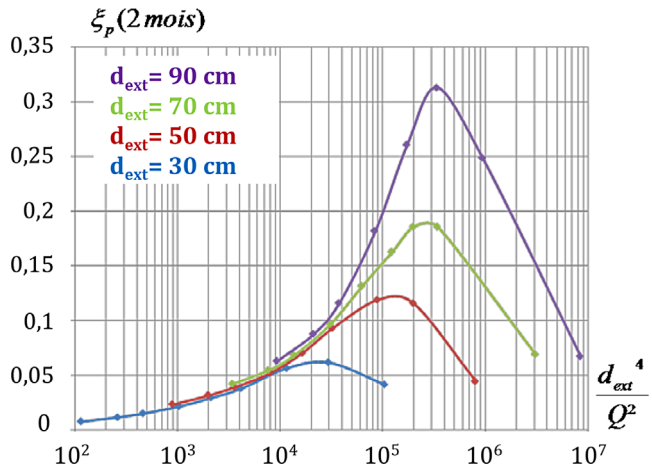

Figure 21. Criterion optimization with the couple (d_{ext}-Q) for two months.

d_{ext} varies from 30 cm to 90 cm length. Others operating and design conditions remain the same than ones defined in Figure 16. Purification is running during two months.

For this specific trap design and with such surface cooling conditions, Figure 21 indicates that hydrogen purification can be optimized with a diameter of 90 cm and a flow rate of 3 m^3/h. This parameters couple is obtained for $\xi_p = 31\,\%$ and $d_{ext}{}^4/Q^2 = 3.10^5 m^2/kg^2$.

CONCLUSION

A model for simulating the sodium purification systems behaviour was developed, integrating the two kinds of crystallization occurring in cold traps. The model describes the crystallization behaviour of sodium hydride and sodium oxide oc curring preferentially in two different zones: respectively, on cold walls, without mesh packing, and on wires of the mesh packing, located in an isothermal area, located down-stream of the cooled zone.

The model apprehends the progression and/or the densification on porous medium, lead by nucleation process. It relies on a strong coupling between impurities crystallization and transfer phenomena.

Simulation tests have illustrated the consequences of thermo-hydraulic conditions on the deposit. Apprehending the coupling of these physical phenomena will, on the one hand, enable to improve the design of future cold traps. On the other hand, it will enable to adapt operating conditions in order to optimize purification requirements and to increase cold trap lifetime expectancy. Simulation analysis revealed that deposit accumulation on walls depends on proper conditions from natural and forced convections. These conditions can be obtained with specific design and given operating parameters. These parameters can be established by maximizing purification criteria according to Richardson number formulation.

In future studies, the model should be validated at the industrial scale by comparison with data sets obtained on operated reactors, such as PSICHOS type cold trap used in Superphenix.

ACKNOWLEDGMENT

This work, developed by CEA and INPT-LGC, was supported by ALSTOM Power Nuclear.

REFERENCES

[1] M. G. Hemanath, C. Meikandamurthy, A. Ashok Kumar, S. Chandramouli, K. K. Rajan, M. Rajan, G. Vaidyanath, G. Padmakumar, P. Kalyannasundaram, B. Raj, *Nuc. Eng. Des*. **2010**, *240*, 2737.

[2] F. A. Kozlov, V. V. Alexeev, P. Yu. Kovalev, V. Ya. Kumaev, V. V. Matyuchin, E. A. Orlova, E. P. Pirogov, A. P. Sorokin, S. I. Shcherbakov, *Atomic Energy* **2012**, *112*.

[3] C. Latgé, "Sodium quality control," *International Conference on Fast Reactors*, Kyoto, Japan 2009.

[4] J. N. Noden, *A general equation for the Solubility of O_2 in liquid Na*, British Report RB/B/B 2500, 1972.

[5] A. Wittingham, *J. Nucl. Mat.* **1976**, *60*, 119.

[6] C. Latgé, *Etude de la cristallisation de l'oxyde de sodium en milieu sodium liquide*, PhD thesis, INPT, Toulouse, France 1981.

[7] D. Feron, *Etudes des mécanismes de la purification du sodium par les pièges froids*, PhD thesis, INPT-Toulouse, France 1979.

[8] C. Saint Martin, C. Latgé, "Mechanism and kinetics of crystallization of NaH in cold traps," *4th LIMET Conference*, Avignon, France, 17–21 October, 1988.

[9] G. Yevick, Fast Reactor Technology, Plant Design, MIT, 1966, p. 224.

[10] A. D. Gadeken, M. C. Plummer, *SEFOR Cold-Trap experience, AEC Research and Development Report*, GEAR-10548, 1972.

[11] D. J. Hebditch, B. J. Gliddon, "Impurity crystallization in liquid sodium systems," *International Conference on Liquid Metal Technology in Energy Production*, CONF-760503-P2, 643, 1976.

[12] C. Latgé, M. Lagrange, M. Suraniti, J. B. Ricard, "Development of a new cold trap concept for Fast Breeder Reactors," *4th LIMET Conference*, 17–21 October, Avignon, France 1988.

[13] M. Rajan, "Sodium removal and requalification of a secondary loop cold trap," *International Working Group of Fast Breeder Reactors* (IWGFR-98), France 1997, p. 3.

[14] M. Boutrais, L. Champeix, P. Chouard, M. Dolias, A. Tibi, "Sodium analysis and purification: aerosols trapping in PHENIX reactor," *Proceedings of the International Conference on Fast Reactor Power Stations*, BNES, London 1974.

[15] C. Latgé, "Etudes des mécanismes et identification des cinétiques de cristallisation de l'oxyde de sodium dans les pièges froids," *3ème Conférence Internationale sur la technologie des métaux liquides pour la production d'énergie*, Oxford 1984.

[16] M. Murase, I. Sumida, K. Kotani, *Nucl. Technol*. **1978**, *37*.

[17] P. Yu, L. G. Basov, T. G. Volchkov, F. A. Zyatchina, F. A. Kozlov, V. P. Kozlov, P. Yu, *J. Eng. Phys. Thermophys*. **1979**, *37*, 1158.

[18] G. Rodriguez, C. Latgé, "The various sodium purification techniques," *International Working Group of Fast Breeder Reactors* (IWGFR-98), France, 3–7 November, 1997.

[19] B. C. Goplen, J. C. Biery, C. C. McPheeters, *Numerical simulation of a cold trap for sodium purification*, University of California, LA-4435, TID-4500, 1970.

[20] C. C. McPheeters, D. J. Raue, "Computer analysis of sodium cold trap design and performance," *Proceedings of the Third International Conference on Liquid Metal Engineering and Technology*, Vol. 1. BNES, London 1984.

[21] K. R. Kim, J. Y. Jeong, K. C. Jeong, S. W. Kwon, S. T. Hwang, *J. Indus. Eng. Chem*. **1998**, *4*, 113.

[22] F. Zhao, X. Ren, *Nucl. Eng. Des*. **2008**, *239*, 490.

[23] V. Ya. Kumaev, V. V. Alekseev, F. A. Kozlov, E. P. Pirogov, "Numerical modeling of impurity mass-transfer in cold traps of BN reactors," *Technology of Alkali Liquid-Metal Coolants: Abstr. Seminar Thermophysics-2009*, GNTs RF–FEI, Obninsk, 2009, p. 64.

[24] C. Latgé, G. Hulme, D. G. Jones, F. Perret, "Experimental studies of packless cold traps for validation of the VICSEN code for prediction of cold trap behaviour," *4th LIMET Conference*, Avignon 1988.

[25] N. Khatcheressian, *Développement d'un modèle de transferts couplés pour l'aide à la conception et à la conduite des systèmes de purification du sodium des réacteurs à neutrons rapides*, PhD thesis, INPT, 2013.

[26] S. Osher, J. A. Sethian, *J. Comput. Phys*. **1988**, *79*, 12.

[27] J. A. Sethian, P. Smereka, *Level Set Methods for Fluid Interfaces, Department of Mathematiques*, universities of California (Berkley) and Michigan (Ann Arbor), http://math.berkeley.edu/.

[28] R. Barnkob, M. Bækbo-Andersen, *Two Phase Flow by Level Set Method*, MIC-Department of Micro and Nanotechonology, Technical University of Denmark, http://web-files.ait.dtu.dk/, 2007.

[29] E. Olsson, G. Kreiss, *J. Comput. Phys*. **2005**, *210*, 225.

[30] C. Beckermann, H. J. Diepers, I. Steinbach, A. Karma, X. Tong, *J. Comput. Phys*. **1999**, *154*, 468.

[31] Y. Sun, C. Beckermann, *Physica. D*. **2004**, *198*, 281.

[32] P. H. Chiu, Y. T. Lin, *J Comput. Phys*. **2011**, *230*, 185.

[33] M. Moguedet, P. Namy, Y. Bereaux, *On the Use of Comsol Multiphysics® to Understand and Optimize the Filling Phase in Injection and Micro-Injection Molding Process*, P.o.t.C. Users, Grenoble 2007.